

Design of Experiments optimisation of Scottish wood biochars and process parameter significance for target applications

Mohammad Umair Jamal (✉ umair.jamal@strath.ac.uk)

University of Strathclyde <https://orcid.org/0000-0001-5005-5817>

Ashleigh J. Fletcher


University of Strathclyde

Research Article

Keywords: Pyrolysis, adsorption, contact angle, activated carbon, wood, surface area

Posted Date: November 10th, 2022

DOI: <https://doi.org/10.21203/rs.3.rs-2209948/v1>

License:  This work is licensed under a Creative Commons Attribution 4.0 International License. [Read Full License](#)

Version of Record: A version of this preprint was published at BioEnergy Research on April 15th, 2023. See the published version at <https://doi.org/10.1007/s12155-023-10595-6>.

Abstract

Biochar production from sustainable materials through pyrolysis remains a key area of research, where additional value can be gained by understanding the influence of initial operating parameters to create optimised carbon products with different characteristics. In this study, native Scottish wood samples were used to produce biochars. Softwood and hardwood samples were investigated to determine feedstock importance, with a focus on the influence of process conditions on the final characteristics of biochars. Screening experiments helped to determine that the softwood feedstock resulted in enhanced product characteristics and identified the optimal pyrolysis temperature. A design of experiments approach was used to scope process variables for softwood feedstock: contact time with activating agent, gas flowrate, and influence of ramp rate during pyrolysis were studied. The response variables were product yield and biochar surface area. As expected, product yield decreased with increasing pyrolysis temperature, and increased ramp rates decreased biochar yield. Pore structure was a combination of micro- and mesopores, and high gas flowrate and pyrolysis temperature produced biochars with the greatest surface areas, while morphological analysis suggests a layered carbon structure. Contact angle analysis suggested hydrophilicity, suggesting compatibility with aqueous media, while a neutral surface charge demonstrates easy application in drinking water treatment systems. The results show the potential of parameter optimisation and insight into the interplay of these variables in biochar development, with characteristics that can be tailored to a range of applications.

1. Introduction

Biochar is the black carbonaceous residue formed from the thermochemical conversion of biomass in an inert atmosphere [1]; these materials need to have similar or superior performance than commercially used activated carbons for their implementation across different applications. This is achieved by a combination of cheap availability of feedstock, accompanied by diverse physical and chemical properties, giving carbon-rich biochars the potential to be used in a range of applications [2], including soil amendment, as enrichment fertilisers [3, 4], catalysts [5], adsorbents [3], and in energy storage [6].

Pyrolysis is frequently used to produce biochars from biomass and wood substrates [2]. The process can be divided into two classes: fast pyrolysis is governed by a high heating rate (10–200°C/s) with a residence time of a few seconds, primarily to produce bio-oils, while slow pyrolysis comprises a lower heating rate (1-100°C/min) with contact times ranging from a few minutes to several days and is the preferred route in biochar production [7, 8]. Surface area and porosity are the commonest determining factors of biochar performance, as the availability of active sites and accessible internal volume govern interaction potentials important in adsorption and cation exchange, while also influencing water holding capacities [9].

Over the years, a plethora of materials have been used to produce carbon-based materials. The abundance of wastes produced from households and agricultural residues, and the feasibility to transform these into carbon materials, has attracted researchers to work towards the concept of a circular economy within biochars production. Biochars have well-developed pore networks, ranging from micro- to macropores, and high surface areas that make them suitable for adsorption [10]. The pore network extends throughout the material and provides active binding sites for heavy metals that readily sorb on the surface and within the pore network. Biochars made from renewable sources gave comparable adsorption capacities to commercial activated carbons, even though the surface areas were significantly smaller [11]. As a consequence of these characteristics, many biochars have been applied in water treatment processes, extending the circularity of their manufacture. Table 1 summarises different feedstock used to produce biochars and their application in water treatment systems.

Table 1
Different feedstock for biochar production and target compounds in water treatment

Feedstock for biochar production	Pollutant species	Reference
Grape bagasse	Copper	[12]
Modified waste potato peels, commercial coffee waste	Cobalt ions, heavy metals	[13, 14]
Walnut wood	Lead and methylene blue	[15]
Rosid angiosperm	Metaldehyde	[16]
Peanut shell	Metal ion	[17]
Anaerobically digested biomass	Heavy metal	[18]
Hazelnut shell	Chromium (VI)	[19]
Apple wastes	Heavy metal	[20]

In addition to water treatment, there are several other areas where biochars have been tested. For example, biochar based acid catalysts derived from rice husk [21], coconut shells [22] and pyrolysed hard wood [23] have found potential application in biodiesel production; biochars as soil enhancement materials can maintain nutrients within soil and control cation exchange, which reduces nutrient leaching from soils [11], while potassium hydroxide activated biochar could be used within supercapacitors [24]. There are several parameters involved in the production of biochars: operating temperature, gas flowrate, residence time, furnace ramp rate, and pressure that can influence the yield and quality of the final product. The influence of these key parameters are outlined below, allowing for variable selection to obtain optimised biochars materials.

Pyrolysis temperature is considered one of the key factors influencing the properties of biochars; the breakdown of heavy hydrocarbons decreases the quantity of the final product, as more volatiles are removed from the system [25]. Many researchers have reported a reduction in biochar yield on increasing the pyrolysis temperature, which is expected [16, 26, 27] as, at high temperatures, secondary reactions occur that further breakdown the char formed at initial temperatures into liquid and gaseous phases, i.e. releasing more volatile components [28]. While higher temperatures enables the development of micropores and an enhanced pore structure [8], a disadvantage of extreme temperatures is that the formation of ash hinders the growth of the pore network and surface area [29], and a fine balance exists in determining the optimal temperature for biochars formation. By contrast, too low a temperature can result in insignificant changes in pore volume and surface area, as the system is unable to completely devolatilise volatile constituents, and the final product may be subject to pore blockage and an underdeveloped pore network [30]. Previous studies indicate that a temperature range between 400 and 800°C is most appropriate for biochar production.

During pyrolysis, vapours are formed, and these can participate in reactions with the char, modifying its characteristics if not purged from the system [28]. Carrier gases are used to ensure an inert atmosphere for pyrolysis, and nitrogen is the most common carrier gas used being cheaper and more readily available than other inert gases. Increased gas flowrate has been shown to marginally decrease the biochar yield, due to the removal of vapours from the system, preventing repolymerisation [28]; previous work has shown a reduction in yield from 28.4% to ~27% on increasing the nitrogen flowrate from 50 to 400 mL/min [31], with similar observations for other systems [12, 32, 33], suggesting that low to moderate flowrates will produce little effect on yield. By contrast, gas flowrate has been shown to markedly affect surface area and total pore volume, with an increase in nitrogen flowrate (50 to 150 mL/min) reported to cause an increase of >300 m²/g in surface area and a ten-fold increase in total pore volume for Algerian date pits derived activated carbon [34]. Notably, very high gas flowrates decrease biochar yield and pore volume [34, 35], hence, moderate gas flowrates between 150 and 300 mL/min are suggested for optimum characteristics.

A low heating rate mitigates the possibility of thermal cracking of biomass and rules out secondary pyrolysis reactions to enhance the biochar yield [28]. A very high heating rate would melt the biochar particles and increase the gaseous and liquid components, thereby decreasing the quantity of the final product [2]. An excessive heating rate also results in accumulation within particles, resulting in blocked pore entrances, due to shortage of time for the volatile matter to diffuse [36], while depolymerisation of biomass and prevalence of secondary pyrolysis result in a reduced biochar yield [37, 38], and can decrease surface area [39]. To avoid micropore coalescence or collapse of the carbon matrix altogether, a high rate of volatile matter generation must be avoided [2], which rules out the use of high heating rates, hence, an optimum range of 10 and 30°C/min is preferred. Residence time is influenced by temperature, gas flowrate and heating rate; to promote repolymerisation, and improve biochar yield, sufficient residence time is necessary for reaction [40], however, several researchers have reported that the yield is not proportional to residence time [41, 42]. Residence times between 30 and 60 min have been reported to yield maximum pore volume for chemically activated biochars from corn cob [43], while an increase in the surface area was reported by for residence time increasing from 10 to 60 min [44]; however further increase reduced surface area. Complications, arising from interaction between other process conditions and residence time, make it a challenging parameter to analyse; hence, it is a key component to investigate during biochar production with residence times between 20 and 60 min being of interest. By contrast the influence of pressure on biochar production is relatively straightforward. Extreme, high pressures prevent the release of volatile matter from the system and result in the formation of spherical cavities [45], with continuous decrease in surface areas reported upon increasing the pressure from 1 to >20 bar [45, 46]. Pressures slightly higher than atmospheric pressure can increase the residence time of reaction constituents, which assists char formation [47], and carbon content in the final product was suggested to be pressure dependent [28]. Feedstock with different physical and chemical compositions, react differently to operational parameters and produce biochars with variability in characteristics [48]. Previous studies have discussed the relationship between biochar performance and process parameters [49, 50]. However, there is a limitation and lack of understanding of simultaneous influence of these parameters on produced biochars. In order to understand the optimal conditions required to produce target characteristics in biochars obtained from waste sources, the effects of these process parameters on biochars produced from Scottish woods were investigated in this study. The raw materials are available in abundance and procured locally, therefore, there is a considerable reduction in carbon footprint associated with supply and transport, offering the potential for circularity in the formation of biochars materials for local applications.

2. Methodology

The wood samples used in this study were procured from Sustainable Thinking Scotland C.I.C. (Kinneil Estate, Bo'ness, Scotland), and obtained from a walled garden in a 200-acre estate. If not used for biochar production, the samples would either be left to decompose within the

woodland, which would result in the eventual release of all of the collected carbon dioxide into the atmosphere or enter Falkirk Council's waste streams to be disposed of via cold composting processes. There have been concerns about cold composting involving ammonia and carbon loss, as well as the overall effectiveness of the process, making production of biochars for subsequent use a viable and green alternative. Wood samples included birch, oak, ash, Scots pine, Sitka spruce and Western red cedar. Table 2 gives an overview of the sample mix used in the study.

Table 2

Feedstock for biochar production

Sample	Wood type	Species
A	predominantly softwood	ash, birch, oak, Scots pine, Sitka spruce, Western red cedar
B	predominantly hardwood	ash, Downey birch, oak, Scots pine, Sitka spruce, Western red cedar
C	100% softwood	Scots pine, Sitka spruce, western red cedar

Samples A and B were developed to give a comparison between biochars produced from soft and hardwoods. A design of experiments (DoE) approach was adopted and based on a comprehensive literature review. Screening experiments were performed on Samples A and B to identify the type of wood to be used for the DoE study. The results of the preliminary runs on Samples A and B were refined and DoE was applied to Sample C. Parameter scoping helped develop DoE runs to investigate a wider parameter space, utilising statistical analysis of variance (ANOVA) to determine responses arising due to multiple factors changing simultaneously [51]. This provides a deeper understanding of the systematic factors that have statistical influence on the chosen responses.

2.1 Design of experiments (DoE)

The screening runs were based on three variables: contact time with activating agent (CO₂), flowrate of activating gas, and furnace temperature. Two temperatures (600 and 850 °C) were chosen based on a review of the literature, to study the difference in the types of produced biochars, as well as yields. Thermal CO₂ activation improves sorption characteristics of biochar and forms new functional groups, creating a more uniform porous structure, and is quicker than chemical activation. Flowrates of 100 or 250 mL/min were used with residence times of 20 and 60 min.

Screening identified softwood as a more desirable feedstock, hence, DoE was applied to pure softwood samples. A mean temperature of 725 °C was used with two variables: contact time and gas flowrate for the full factorial design (FFD). FFD resulted in a total of $2^2 = 4$ experiments for 2 factors with a high and low setting each [52]. DoE experiments were conducted at a ramp rate of 15 °C/min and an additional set of 4 experiments was conducted under similar conditions, with the ramp rate increased to 30 °C/min to analyse the effect on biochar properties. A precursor weight of 30 ± 0.1 g was chosen for both screening and experimental runs to ensure sufficient yield for subsequent analysis.

2.2 Nomenclature

Sample names were developed according to: the first three digits (e.g., 250 or 100) represent the gas flowrate. 'S' and 'H' denote either softwood or hardwood; the middle set of values (600, 850, 725) represent the pyrolysis temperatures; followed by residence time and sample category, e.g. 20A or 60C. Thus, the sample 250S725-60C represents a gas flowrate of 250 mL/min, for a softwood sample pyrolysed at 725 °C with a residence time of 60 min, from wood batch C. All experiments were conducted at a heating rate of 15 °C/min, with the exception of samples marked '/30', where the ramp rate was increased to 30 °C/min.

2.3 Pyrolysis

Prior to combustion, the wood samples were divided into cubes of sides ~5 cm, as shown in Figure 1. These smaller cubes were washed with de-ionised water to remove dust and oven dried at 100 °C for 24 h. For combustion, a precursor weight of 30 ± 0.1 g was used. The sample was equally distributed into four crucibles fitted with lids, all placed inside the Thermconcept KLS 10/12/WS muffle furnace, as shown in Figure 2. A CO₂ flow of 250 mL/min was maintained over the sample for 40 min to ensure an inert atmosphere, and the furnace set to the corresponding temperature and dwell time. Following this, the gas flowrate was adjusted to the values detailed in Tables 3 and 4 and heating begun. After each run was complete, the flow of gas was switched off once the furnace reached room temperature and the sample was allowed to cool overnight. Figure 3 shows a schematic diagram of the muffle furnace used for pyrolysis.

Biochar weight was calculated once the samples had reached room temperature. The yield of the sample was calculated using Equation 1:

$$\text{Biochar yield (\%)} = \frac{\text{produced biochar weight (g)}}{\text{precursor weight (g)}} * 100 \quad [1]$$

2.4 Analysis and Characterisation

Porous structure characterisation The biochar sample was crushed to a powdered form prior to analysis, performed using nitrogen adsorption at -196 °C on a Micrometrics ASAP 2420 system (99.99 % nitrogen adsorbate). Degas was performed at 200 °C for 240 min (10 °C/min heating rate). A total of 49 points were taken on the adsorption branch and 30 on the desorption branch. Specific surface area and pore volume distribution of the samples was determined using Brunauer-Emmett-Teller (BET) model (Reichenauer and Scherer, 2000, IUPAC, 1985).

Fourier transform infrared spectroscopy (FTIR) The biochars were crushed to a powdered form, and a small amount of sample (~ 0.2 g) was placed on the sampling surface. An ABB IR Instrument MB 300 series was used to characterise the functional groups on the surface of the biochar samples using Attenuated Total Reflectance (ATR) for analysis. A total of 32 scans were taken in transmittance mode. The spectra were recorded at 4 cm⁻¹ resolution between 500 and 4000 cm⁻¹.

Proximate analysis Thermogravimetry was used to carry out proximate analysis of representative biochar samples. The technique employed closely follows the British Standard (BS1016) method. Approximately 5-10 mg of crushed sample was placed in a crucible and analysed using a Stanton Redcroft STA 780 series thermogravimetric analyser. The crucible was initially tared under a nitrogen gas flow of 50 mL/min, and the mass allowed to stabilise under the same gas flowrate and initial mass recorded. The sample was heated to 393 K and allowed to stabilise. Subsequently, crucible mass was recorded, and the temperature increased to 1193 K (50 K/min ramp rate), and held for 3 min, before the mass reading was recorded. Finally, the temperature was reduced to 1093 K and the flowing gas switched to 50 mL/min of pressurised air. The crucible was allowed to stabilise, and a final mass reading was taken at ambient temperature.

Scanning electron microscopy (SEM) SEM was used to capture the structural characteristics of the biochar surface. A small solid portion was clipped from a biochar cube and placed into the apparatus (Tungsten low-vacuum JEOL JSM-IT100 InTouchScope SEM). Images were captured at 10 µm with x1000 magnification. The beam current was kept constant at 35 with a voltage difference of 20 kV.

Point of zero charge (PZC) A salt addition method was used to perform PZC analysis [53]. A 40 mL aliquot of 0.1M NaNO₃ was adjusted to five pH values between 3 and 11. Solutions of 0.1M NaOH and 0.1M HCl were used to attain the desired pH. Powdered biochar (~0.2 g) was added to the beakers and agitated at 450 rpm for 24 h. The final solution was filtered and the pH of the permeate was measured. The difference between the initial and final pH values of the samples was calculated and the change in pH versus initial value was plotted to identify the PZC.

Contact angle measurement A sessile drop method was used to determine the contact angle between the biochar surface and a water drop. Biochar samples were crushed, and a small amount of powder was placed on a microscopic glass slide. The lump was then smoothed by placing another slide on top which was removed before taking measurements. Analysis was performed on a Krüss Scientific Drop Shape Analyser DSA25B. To measure the contact angle, a small droplet of water (~0.5 mL) was dropped onto the sample from a height less than 1 cm, and photographs were taken at intervals of 1, 2 and 3 seconds using Krüss Advance software.

3. Results And Discussion

Table 3

Process conditions, yields and textural properties for biochars produced using wood samples A and B (Ramp rate = 15°C/min)

Exp	Sample code	CO ₂ flowrate (mL/min)	Temp (°C)	Contact time (min)	Biochar weight (g)	Yield (%)	Surface Area (m ² /g)	Micropore Volume (cm ³ /g)	Total pore volume (cm ³ /g)	Average pore width (nm)
S1	250S600-20A	250	600	20	6.53	21.8%	544	0.18	0.26	3
S2	250S600-60A	250	600	60	6.20	20.7%	538	0.18	0.25	3
S3	250S850-20A	250	850	20	5.30	17.7%	597	0.20	0.29	3
S4	100S850-60A	100	850	60	4.41	14.7%	764	0.22	0.42	5
S5	250H600-20B	250	600	20	7.59	25.3%	525	0.17	0.25	3
S6	250H600-60B	250	600	60	6.96	23.2%	544	0.18	0.27	3
S7	250H850-20B	250	850	20	5.16	17.2%	573	0.19	0.26	3
S8	100H850-60B	100	60	100	4.54	15.1%	714	0.23	0.34	4

Table 4

Process conditions, yields and textural properties for biochars produced wood sample C

Exp	Sample code	CO ₂ flowrate (mL/min)	Temp (°C)	Contact time (min)	Biochar weight (g)	Yield (%)	Surface Area (m ² /g)	Micropore Volume (cm ³ /g)	Total pore volume (cm ³ /g)	Average pore width (nm)	Fixed carbon (%)	Volatile matter (%)
Feedstock											20.3	79.7
Ramp rate = 15°C/min												
D1	250S725-60C	250	725	60	5.30	17.7%	613	0.19	0.36	3	80.0	20.0
D2	100S725-60C	100	725	60	5.27	17.6%	613	0.19	0.35	3	86.0	14.0
D3	250S725-20C	250	725	20	6.08	20.3%	558	0.18	0.29	4	80.5	19.5
D4	100S725-20C	100	725	20	6.31	21.0%	581	0.19	0.29	5	80.0	20.0
Ramp rate = 30°C/min												
D5	250S725-60/30C	250	725	60	4.40	14.7%	613	0.19	0.37	5	77.3	22.7
D6	100S725-60/30C	100	725	60	3.65	12.2%	553	0.18	0.43	4	73.4	26.6
D7	250S725-20/30C	250	725	20	6.08	20.3%	544	0.18	0.27	4	85.1	14.9
D8	100S725-20/30C	100	725	20	6.07	20.2%	544	0.17	0.28	4	83.5	16.5

3.1 Biochar yield

Table 3 shows the percentage yield of biochars produced from screening wood samples A and B, under different pyrolysis temperatures and operating parameters. The trend in yield is as expected, with increasing pyrolysis temperatures resulting in lower quantities of produced biochars [16, 26, 27]. As the temperature is increased, more volatiles are removed from the system, thereby reducing the biomass within the system, hence, the final mass of the biochar. It is evident that the final product is determined by a direct combination of the operating parameters. For the softwood chars (Sample A), a low contact time of 20 min and pyrolysis temperature of 600°C, with a high gas flowrate of 250 mL/min, resulted in the highest biochar yield of 6.53 g. Increasing the contact time to 60 min and keeping the other two parameters constant, resulted in a minor reduction in yield of less than 1%. The result suggests that the increment of contact time from 20 to 60 min does not have a significant impact on the product yield. A similar pattern was observed for the hardwood chars (Sample B). A maximum yield of 7.59 g was obtained using a high gas flowrate, low pyrolysis temperature and low contact time. The yield decreased slightly with increased contact time (~ 2%). The lowest yield was obtained at a temperature of 850°C, with a 60 min residence time and low gas flowrate. Under similar conditions, hardwood samples gave higher yields than the softwood samples. For Experiment S1, the softwood yield was 21.8%, and the hardwood biochar was 25.3% under similar parameters (S5). The difference in yield was not considerable for the other runs in both wood batches. This observation, combined with the specific surface areas obtained, indicated that 100% softwood samples were worthy of further investigation.

Table 4 shows the yield of produced biochars from DoE runs. In D1-4, temperature was fixed at 725°C as an average between the two screening temperatures, and the ramp rate was kept at 15°C/min. A contact time of 60 min, with both gas flowrates, gave an average yield of ~ 17.5%. This yield was slightly improved when the contact time was reduced to 20 min, giving ~ 20%. The ramp rate was increased to 30°C/min for D5-8; combined with a high contact time, the yield was further reduced for runs 13 and 14 [2]. The high heating rate however did not seem to affect the yield with shorter residence times. The data suggests that temperature is the primary factor affecting the yield of biochars. There is a noticeable influence of activating gas residence time and flowrate on the yield, although not as significant. It is therefore necessary to analyse the influence of these parameters on the other response variables as well.

3.2 Porous structure characterisation

Figure 4a and b shows the adsorption isotherms recorded in the screening study. Experiments S1-4 represent a Type II isotherm, governed by adsorption onto microporous solids [54, 55]. The hardwood samples in Experiments S5-8 also display an initial high uptake followed by a plateau. There is slight evidence of a final uptake at high relative pressure, which could be attributed to a Type II isotherm and multilayer adsorption [54, 55].

Adsorption isotherms obtained for the DoE biochars presented in Fig. 4c and d demonstrate a more prevalent Type II/IVa isotherm behaviour with initial high uptakes, followed by a plateau and a slight update at high relative pressure [55]. In general, the evidence of mesoporous nature is more prominent in pure softwood samples (Sample C) in the latter experiments.

Table 3 shows the textural data obtained for the screening samples, comprising the surface area, micropore and total pore volumes, as well as the average pore widths. Similar data on DoE samples is reported in Table 4. Total pore volume of samples was calculated using Eq. 2:

$$\text{Totalporevolume (TPV)} = (Q_{Sat} * MW / V_m) / \rho_{liq} \quad [2]$$

Where, Q_{sat} = maximum nitrogen adsorption (in cm^3/g , usually at relative pressure of 0.97 or above)

MW = molecular weight of N_2 (28 g/mol)

V_m = volume occupied by 1 mole of gas (22.4 L)

ρ_{liq} = Density of liquid N_2 at boiling point (808 g/L)

t plot analysis, developed by Lippens and Boer [56] was used to determine the micropore volumes reported in Tables 3 and 4. It can be inferred that increasing pyrolysis temperatures caused an increase in microporosity. The ratio of micropore volume to TPV is highest in samples with low gas flowrates and higher residence times. At high gas flowrates, $V_{\text{micropore}}/V_{\text{total}}$ ratios are similar for experiments with 20 min hold time at high temperature. The evidence suggests an inverse relationship between microporosity development and residence time. Microporosity is suitable for interactions between small adsorbate species and adsorbents [16], so can be a useful quantity to optimise. DoE Experiments D5 and D6 indicate that a higher ramp rate combined with a longer hold time can enhance mesoporous nature in the biochars, which have previously been shown to be useful for aqueous phase applications [57].

Surface areas were calculated using BET analysis, however, such analysis is highly sensitive to the selected relative pressure range [58], particularly for microporous materials and the optimal relative pressure range can be determined using the four consistency criteria suggested

by Rouquerol *et al.* [59]:

1. Only the range where the product of the adsorbate loading rate and 1 minus the relative pressure is increasing monotonically with the relative pressure should be chosen.
2. The value of BET 'C constant' must be positive. C constant quantifies the adsorbent and adsorbate interactions and is related to the energetics of adsorption in the first adsorbed layer [58].
3. The selected linear region should encompass monolayer loading corresponding to the relative pressure.
4. The relative pressure calculated in Criterion 3. should be equal to the one calculated from BET theory consonant with monolayer loading with a 20% tolerance.

Given the presence of significant microporosity reported in Tables 3 and 4, the Rouquerol correction was applied for all samples produced in this study. Maximum BET surface area was recorded for a pyrolysis temperature of 850°C with a gas flowrate of 100 mL/min and 60 min residence time with softwood precursor (S4). Shorter residence times produced biochars with lower surface areas compared to those obtained under similar conditions but with longer hold time. Similar observations of improved surface areas with residence time were reported previously [44]. On average, pyrolysis runs performed at 725°C produced biochars with higher surface areas. The intermediate temperatures also offered a reasonable trade-off between biochar yield and average pore widths. For DoE runs, high gas flowrate and residence time can be inferred to be directly proportional to surface area. A reduction in $V_{\text{micropore}}/V_{\text{total}}$ ratio of these samples also suggests a more openly porous structure [16]. The highest biochar surface areas obtained for 100% softwood chars were higher than other wood based biochars reported in the literature [16, 60, 61].

Pore width data obtained from Barrett-Joyner-Halenda (BJH) analysis [62] (Tables 3 and 4) further confirms the predominantly microporous nature of the biochars. Average pore widths were greatest for runs performed at 725°C with high ramp rates. As stated above, shorter hold times resulted in greater microporosity, as well as smaller pore widths. Predominantly softwood biochars (S1-4) were almost as microporous as hardwood biochars (S5-8), and Sample C (entirely softwood, D1-8) demonstrated the highest mesoporosity. The results indicate a possible application for Sample A in the adsorption of small adsorptive species, mainly in gas phase [63, 64]; including in carbon capture [54, 65].

3.3 Fourier Transform Infrared Spectroscopy

Figure 5a presents the FTIR spectrum obtained for softwood feedstock. In the fingerprint region, between 600–1500 cm^{-1} , there is evidence of $\text{CH}=\text{CH}_2$ vinyl terminals [66]. There is also evidence of loss of the peak from C-OH vibrations in the feedstock at 1000 cm^{-1} from pyrolysis treatment [16]. The heat treatment plays a crucial role in condensation of the carbonaceous skeleton and removes the hydroxyl groups from cellulosic compounds present in the precursors [67].

Figure 5b and c shows the FTIR spectra for DoE biochar samples obtained using low and high ramp rates. The observed spectra looks identical and not influenced by the change in ramp rates of the experimental runs. The peaks observed between regions 3800 and 3500 cm^{-1} indicate the presence of hydrogen bonds. This information is further supplemented by peaks between 1600 and 1300 cm^{-1} , as is the case with analysed biochar samples [66]. There are sharp peaks from the biochars between 3000 and 2600 cm^{-1} that could be due to C-H stretching bonds [16]. There is also strong evidence of C = C bonds with symmetric and asymmetric vibrations and possible conjugation, as well as stretching vibrations with other structures such as oxygen and hydrogen (C = O, C-H) from the spectra in the 1600–1800 cm^{-1} region [66, 68]. These functional groups could be the result of the presence of ketones, aldehydes and carboxylic acids [69]. The results indicate the development of a layered, almost graphene-like carbon arrangement in the aromatic and aliphatic structures of the biochars [4]. There is no quantifiable influence of gas flowrate and residence time on the functional groups present in the samples. It can therefore be noted that temperature continues to be the primary influence on surface chemistry of produced biochars.

3.4 Proximate Analysis

The dry ash compositions of the feedstock and DoE biochars obtained from thermogravimetric analysis are reported in Table 4. The samples were treated on a dry basis to remove variability from moisture content, and on an ash-free basis due to variability in inorganic forms from the natural precursor. A high gas flowrate in Experiment D1 resulted in a fixed carbon percentage of 80% and a volatile matter content of 20%. This was a significant increase from the fixed carbon content of 20.3% in the feedstock. For Experiment D2, under a much lower gas flowrate, the carbon content was increased to 86% and volatiles reduced to 14%. The higher gas flowrate appears to have potentially decreased the temperature of the sample and affected the release of volatile matter as suggested previously [34, 35]. For Experiments D3 and D4, with shorter residence time, gas flowrates did not have a considerable impact on fixed carbon and volatile fractions. High heating rates combined with longer residence times, result in accumulation of volatile matter [36]. The results obtained in D5 and D6 support this statement, with carbon percentages below 80 and higher volatile content, as opposed to their lower ramp rate counterparts. With a shorter hold period (D7 and D8), the percentages of volatiles reduced significantly and a positive effect on fixed carbon content was also noted. Residence time was observed to be the key driver for fixed carbon and volatiles, with the fluctuations arising from variable gas flowrates being almost negligible. The results

indicate that a higher ramp rate combined with a short residence time has the potential to produce biochars with high fixed carbon content and the lowest fraction of volatiles, albeit with a significant loss in yield.

3.5 Scanning Electron Microscopy

Figure 6a-d show the SEM images recorded for lower ramp rate biochars and e-g display the observations for higher ramp rate biochars. There is evidence of a well-developed pore network in biochars produced at low and high ramp rates. The images at 10 μm and 1000x magnification suggest that the high pyrolysis temperatures exposed the carbonaceous skeleton of the parent material encompassing an intricate network of pores [70]. A pyrolysis temperature that is sufficiently high is necessary for the removal of the outer biochar layer. The open structure of pores could be attributed to a lower ash content, which reduces the potential for clogging. There is no apparent evidence of influence from different ramp rates on the pore networks developed in the biochars.

3.6 Point of Zero Charge

Table 5 shows the point of zero charge (PZC) obtained for biochars used for the DoE study. The surface charge of chars produced under different operating conditions appears to be more dependent on material origin and surface functional groups, as opposed to chosen DoE variables. Pyrolysis temperatures also influence the pH of wood-based biochars. High temperatures result in the loss of not only volatile matter but also acidic functional groups i.e., phenols and carboxylic, thereby resulting in more alkaline surface charges [71]. For example, slow pyrolysis treatment of wood-based pellets at 200°C produced biochars with pH 4.6. Upon increasing the temperature to 600°C, the resulting biochar had a pH of 9.5 [72]. A similar observation on wood chip biochars pyrolysed at 500°C was made with biochars having a pH(H₂O) of 8.58 \pm 0.01 [73]. The average PZC of the samples in this study was 7.40 \pm 0.02, indicating potential application of these biochars to drinking water treatment systems without considerable pH alternation to target anionic species from effluents and treatment systems, or for cationic species by slightly reducing the system pH [71].

Table 5
Point of zero charge of DoE biochars

Sample	100S725-20C	100S725-60C	250S725-20C	250S725-60C
PZC	7.47	7.31	7.38	7.44

3.7 Contact angle measurement

Biochar wettability is a parameter that can be evaluated through contact angle (CA) measurement [74]. Figure 7(a) shows water droplet on a clear glass slide and 7(b) shows a similar water droplet on a biochar film. Both images were taken 2 seconds after water contact. The measurement was repeated for all biochar samples and yielded similar observations. The absorption of water by prepared biochars was seemingly immediate, indicating hydrophilicity and high wettability [74]. Low CA (typically < 90°) are achieved in cases where water shows greater affinity to the solid surface [75]. The mechanism for this interaction could potentially be the formation of surface hydrogen bonds and the domination of adhesion forces over repulsive ones. This stabilisation of forces allows water to penetrate porous materials and wet larger surface areas [74]. This observed wettability in case of native Scottish biochars suggests a feasible application in drinking water treatment systems, allowing larger available surface areas for interaction between dissolved target species in water.

3.8 Discussion

Examination of the wide range of results obtained for the chars produced within this study suggests significant correlation of biochar properties with parameters used within their production. Table 6 provides comparative data for biochars produced from wood-based feedstocks reported in literature, detailing pyrolysis temperatures, surface areas and fixed carbon contents. The surface areas of biochars reported in this study are higher than those produced at similar temperatures, as shown in Table 6. The amount of fixed carbon in wood-based chars appears to be consistent, at around 80%, which was also observed for the DoE biochars. Temperatures above 400°C were reported to produce a recalcitrant structure resulting from the loss of volatile matter, as well as alkyl and carboxylic groups [61]. The statement further supplements the chemical moiety information obtained from FTIR, suggesting a layered carbon structure. The concentric arrangement of pores in the carbonaceous skeleton is also visible in the SEM images.

Table 6
Surface areas and pyrolysis temperatures of biochars produced from wood-based feedstocks

Feedstock	Pyrolysis temperature (°C)	Surface area (m ² /g)	Carbon content (%)	Reference
Oak wood	350	450	-	[76]
	650	642		
Mulberry wood	350	16.6	67.9	[77]
	450	31.5		
	550	58.0		
Hardwood	450	0.43	53.4	[78]
Grey dogwood	755	422	73.1	[79]
Black locust	755	442	72	
Hackberry	755	369	69.9	
Red bud	755	320	71.6	
American linden	755	190	71.2	
Apple tree branch	600	209	81.5	[61]
	700	419	82.3	
	800	545	84.8	
Oak tree	600	289	81.2	
	700	336	83.2	
	800	398	82.9	
Fir wood chips	600	545	89.3	[80]
	700			

Higher temperatures have also been reported to increase alkalinity of biochars [71]. DoE biochars in this work were determined to have an average PZC of 7.40 ± 0.02 . In addition to a neutral pH, contact angle analysis of the biochars suggested hydrophilic character. Rattanakam *et al.* investigated the difference in hydrophilicity of oxidised and un-oxidised wood based biochars [81], reporting an increase in the hydrophilic behaviour of oxidised biochars. Fir wood derived biochars for perchlorate adsorption were contrastingly reported to provide a hydrophobic environment, as opposed to the hydrophilic biochars produced in this work [80]. The high surface areas, carbon content and hydrophilic nature of the biochars produced in this work gives them great potential for possible application in water and wastewater treatment systems [71]. Process parameter influence on biochar characteristics appears to be significant, as evidenced by the DoE study and could potentially provide a pathway to produce sustainable biochars catered to specific applications.

4. Conclusions

Biochars produced from native Scottish woods showed significant influence of pyrolysis operating parameters on the characteristics of the final products. Screening experiments showed that softwood biochars exhibited high surface areas with a slight decrease in yield, as opposed to hardwood biochars. Higher surface areas were obtained with increasing pyrolysis temperatures and high gas flowrates, providing sufficient residence time was allowed, and this was observed for biochars obtained through both screening experiments, as well as the follow-up design of experiments runs. A high residence time not only produced an increase in observed surface area but also appeared to enhance mesoporosity within the pore structure. Biochars obtained using optimised conditions gave the largest surface areas with comparable yield to the screening samples. Porous structure analysis indicates development of mesopores, in tandem with microporosity, within these samples, while higher ramp rates had an adverse effect on biochar yield but improved mesoporous character. Spectroscopic analysis indicates the presence of a layered carbon structure in the biochars. The intricate pore network and graphene like layered porous arrangement is also evident from morphological analysis. A high fixed carbon content resulted from use of a high gas flowrate and longer hold periods with the activating gas. All biochars carry an almost neutral surface charge with a hydrophilic nature, indicating potential for application in water treatment systems. The results demonstrate the potential and importance of varying manufacturing operating parameters to produce biochars catered to specific applications, such as adsorption of pollutants, soil remediation or carbon capture.

Declarations

Conflict of Interests The authors declare no competing interests.

References

1. Sun, Y., et al., *Effects of feedstock type, production method, and pyrolysis temperature on biochar and hydrochar properties*. Chemical Engineering Journal, 2014. **240**: p. 574-578.
2. Leng, L., et al., *An overview on engineering the surface area and porosity of biochar*. Science of The Total Environment, 2021. **763**: p. 144204.
3. Manyà, J.J., *Pyrolysis for Biochar Purposes: A Review to Establish Current Knowledge Gaps and Research Needs*. Environmental Science & Technology, 2012. **46**(15): p. 7939-7954.
4. Ahmad, M., et al., *Biochar as a sorbent for contaminant management in soil and water: A review*. Chemosphere, 2014. **99**: p. 19-33.
5. Lee, J., K.-H. Kim, and E.E. Kwon, *Biochar as a Catalyst*. Renewable and Sustainable Energy Reviews, 2017. **77**: p. 70-79.
6. Liu, W.-J., H. Jiang, and H.-Q. Yu, *Emerging applications of biochar-based materials for energy storage and conversion*. Energy & Environmental Science, 2019. **12**(6): p. 1751-1779.
7. Kan, T., V. Strezov, and T.J. Evans, *Lignocellulosic biomass pyrolysis: A review of product properties and effects of pyrolysis parameters*. Renewable and Sustainable Energy Reviews, 2016. **57**: p. 1126-1140.
8. Lehmann, J. and S. Joseph, *Biochar for Environmental Management*. 2nd ed. 2015, London: Routledge. 976.
9. Weber, K. and P. Quicker, *Properties of biochar*. Fuel, 2018. **217**: p. 240-261.
10. Mukherjee, A., A.R. Zimmerman, and W. Harris, *Surface chemistry variations among a series of laboratory-produced biochars*. Geoderma, 2011. **163**(3): p. 247-255.
11. Ahmad, J., et al., *Exploring untapped effect of process conditions on biochar characteristics and applications*. Environmental Technology & Innovation, 2020. **21**: p. 101310.
12. Demiral, H. and C. Güngör, *Adsorption of copper(II) from aqueous solutions on activated carbon prepared from grape bagasse*. Journal of Cleaner Production, 2016. **124**: p. 103-113.
13. Kyzas, G.Z., E.A. Deliyanni, and K.A. Matis, *Activated carbons produced by pyrolysis of waste potato peels: Cobalt ions removal by adsorption*. Colloids and Surfaces A: Physicochemical and Engineering Aspects, 2016. **490**: p. 74-83.
14. Kyzas, G.Z., *Commercial Coffee Wastes as Materials for Adsorption of Heavy Metals from Aqueous Solutions*. Materials, 2012. **5**(10): p. 1826-1840.
15. Ghaedi, M., et al., *Application of central composite design for simultaneous removal of methylene blue and Pb²⁺ ions by walnut wood activated carbon*. Spectrochimica Acta Part A: Molecular and Biomolecular Spectroscopy, 2015. **135**: p. 479-490.
16. Idowu, G.A. and A.J. Fletcher, *The Manufacture and Characterisation of Rosid Angiosperm-Derived Biochars Applied to Water Treatment*. BioEnergy Research, 2020. **13**(1): p. 387-396.
17. Wilson, K., et al., *Select metal adsorption by activated carbon made from peanut shells*. Bioresource Technology, 2006. **97**(18): p. 2266-2270.
18. Inyang, M., et al., *Removal of heavy metals from aqueous solution by biochars derived from anaerobically digested biomass*. Bioresource Technology, 2012. **110**: p. 50-56.
19. Cimino, G., A. Passerini, and G. Toscano, *Removal of toxic cations and Cr(VI) from aqueous solution by hazelnut shell*. Water Research, 2000. **34**(11): p. 2955-2962.
20. Marañón, E. and H. Sastre, *Heavy metal removal in packed beds using apple wastes*. Bioresource Technology, 1991. **38**(1): p. 39-43.
21. Li, M., D. Chen, and X. Zhu, *Preparation of solid acid catalyst from rice husk char and its catalytic performance in esterification*. Chinese Journal of Catalysis, 2013. **34**(9): p. 1674-1682.
22. Hidayat, A., et al., *Esterification of Palm Fatty Acid Distillate with High Amount of Free Fatty Acids Using Coconut Shell Char Based Catalyst*. Energy Procedia, 2015. **75**: p. 969-974.
23. Dehkoda, A.M., A.H. West, and N. Ellis, *Biochar based solid acid catalyst for biodiesel production*. Applied Catalysis A: General, 2010. **382**(2): p. 197-204.
24. Dehkoda, A.M., N. Ellis, and E. Gyenge, *Electrosorption on activated biochar: effect of thermo-chemical activation treatment on the electric double layer capacitance*. Journal of Applied Electrochemistry, 2014. **44**(1): p. 141-157.

25. Roncancio, R. and J.P. Gore, *CO₂ char gasification: A systematic review from 2014 to 2020*. Energy Conversion and Management: X, 2021. **10**: p. 100060.
26. Pütün, A.E., A. Özcan, and E. Pütün, *Pyrolysis of hazelnut shells in a fixed-bed tubular reactor: yields and structural analysis of bio-oil*. Journal of Analytical and Applied Pyrolysis, 1999. **52**(1): p. 33-49.
27. Ateş, F., E. Pütün, and A.E. Pütün, *Fast pyrolysis of sesame stalk: yields and structural analysis of bio-oil*. Journal of Analytical and Applied Pyrolysis, 2004. **71**(2): p. 779-790.
28. Tripathi, M., J.N. Sahu, and P. Ganesan, *Effect of process parameters on production of biochar from biomass waste through pyrolysis: A review*. Renewable and Sustainable Energy Reviews, 2016. **55**: p. 467-481.
29. Luo, L., et al., *Properties of biomass-derived biochars: Combined effects of operating conditions and biomass types*. Bioresource Technology, 2015. **192**: p. 83-89.
30. Pallarés, J., A. González-Cencerrado, and I. Arauzo, *Production and characterization of activated carbon from barley straw by physical activation with carbon dioxide and steam*. Biomass and Bioenergy, 2018. **115**: p. 64-73.
31. Ertaş, M. and M. Hakkı Alma, *Pyrolysis of laurel (Laurus nobilis L.) extraction residues in a fixed-bed reactor: Characterization of bio-oil and bio-char*. Journal of Analytical and Applied Pyrolysis, 2010. **88**(1): p. 22-29.
32. Heidari, A., et al., *Effect of process conditions on product yield and composition of fast pyrolysis of Eucalyptus grandis in fluidized bed reactor*. Journal of Industrial and Engineering Chemistry, 2014. **20**(4): p. 2594-2602.
33. Zhang, H., et al., *Comparison of non-catalytic and catalytic fast pyrolysis of corncob in a fluidized bed reactor*. Bioresource Technology, 2009. **100**(3): p. 1428-1434.
34. Bouchelta, C., et al., *Effects of pyrolysis conditions on the porous structure development of date pits activated carbon*. Journal of Analytical and Applied Pyrolysis, 2012. **94**: p. 215-222.
35. Lua, A.C., F.Y. Lau, and J. Guo, *Influence of pyrolysis conditions on pore development of oil-palm-shell activated carbons*. Journal of Analytical and Applied Pyrolysis, 2006. **76**(1): p. 96-102.
36. Angin, D., *Effect of pyrolysis temperature and heating rate on biochar obtained from pyrolysis of safflower seed press cake*. Bioresource Technology, 2013. **128**: p. 593-597.
37. Aysu, T. and M.M. Küçük, *Biomass pyrolysis in a fixed-bed reactor: Effects of pyrolysis parameters on product yields and characterization of products*. Energy, 2014. **64**: p. 1002-1025.
38. Şensöz, S. and D. Angin, *Pyrolysis of safflower (Charthamus tinctorius L.) seed press cake: Part 1. The effects of pyrolysis parameters on the product yields*. Bioresource Technology, 2008. **99**(13): p. 5492-5497.
39. Chen, D., et al., *Pyrolysis polygeneration of poplar wood: Effect of heating rate and pyrolysis temperature*. Bioresource Technology, 2016. **218**: p. 780-788.
40. Park, H.J., Y.-K. Park, and J.S. Kim, *Influence of reaction conditions and the char separation system on the production of bio-oil from radiata pine sawdust by fast pyrolysis*. Fuel Processing Technology, 2008. **89**(8): p. 797-802.
41. Mohamed, A.R., et al., *The Effects of Holding Time and the Sweeping Nitrogen Gas Flowrates on the Pyrolysis of EFB using a Fixed-Bed Reactor*. Procedia Engineering, 2013. **53**: p. 185-191.
42. Tsai, W.T., M.K. Lee, and Y.M. Chang, *Fast pyrolysis of rice husk: Product yields and compositions*. Bioresource Technology, 2007. **98**(1): p. 22-28.
43. Tsai, W.T., C.Y. Chang, and S.L. Lee, *Preparation and characterization of activated carbons from corn cob*. Carbon, 1997. **35**(8): p. 1198-1200.
44. Zhao, B., et al., *Effect of pyrolysis temperature, heating rate, and residence time on rapeseed stem derived biochar*. Journal of Cleaner Production, 2018. **174**: p. 977-987.
45. Cetin, E., R. Gupta, and B. Moghtaderi, *Effect of pyrolysis pressure and heating rate on radiata pine char structure and apparent gasification reactivity*. Fuel, 2005. **84**(10): p. 1328-1334.
46. Melligan, F., et al., *Pressurised pyrolysis of Miscanthus using a fixed bed reactor*. Bioresource Technology, 2011. **102**(3): p. 3466-3470.
47. Manyà, J.J., F.X. Roca, and J.F. Perales, *TGA study examining the effect of pressure and peak temperature on biochar yield during pyrolysis of two-phase olive mill waste*. Journal of Analytical and Applied Pyrolysis, 2013. **103**: p. 86-95.
48. Rehrah, D., et al., *Short-term greenhouse emission lowering effect of biochars from solid organic municipal wastes*. International Journal of Environmental Science and Technology, 2018. **15**(5): p. 1093-1102.
49. Hassan, M., et al., *Influences of feedstock sources and pyrolysis temperature on the properties of biochar and functionality as adsorbents: A meta-analysis*. Science of The Total Environment, 2020. **744**: p. 140714.

50. Leng, L. and H. Huang, *An overview of the effect of pyrolysis process parameters on biochar stability*. Bioresource Technology, 2018. **270**: p. 627-642.
51. Deloach, R. *Analysis of Variance in the Modern Design of Experiments*. American Institute of Aeronautics and Astronautics.
52. Barad, M., *Design of Experiments (DOE)—A Valuable Multi-Purpose Methodology*. Applied Mathematics, 2014. **05**(14): p. 2120-2129.
53. Bakatula, E.N., et al., *Determination of point of zero charge of natural organic materials*. Environmental Science and Pollution Research, 2018. **25**(8): p. 7823-7833.
54. IUPAC, *Reporting Physisorption Data for Gas/Solid systems*. International Journal of Pure and Applied Chemistry (IUPAC), 1985. **57**: p. 603-619.
55. Thommes, M., et al., *Physisorption of gases, with special reference to the evaluation of surface area and pore size distribution (IUPAC Technical Report)*. Pure and applied chemistry, 2015. **87**(9): p. 1051-1069.
56. Lippens, B.C. and J.H. de Boer, *Studies on pore systems in catalysts: V. The t method*. Journal of Catalysis, 1965. **4**(3): p. 319-323.
57. Parsa, M., et al., *Biochars derived from marine macroalgae as a mesoporous by-product of hydrothermal liquefaction process: Characterization and application in wastewater treatment*. Journal of Water Process Engineering, 2019. **32**: p. 100942.
58. Gómez-Gualdrón, D.A., et al., *Application of Consistency Criteria To Calculate BET Areas of Micro- And Mesoporous Metal–Organic Frameworks*. Journal of the American Chemical Society, 2016. **138**(1): p. 215-224.
59. Sing, K.S.W., *7 - Assessment of Surface Area by Gas Adsorption*, in *Adsorption by Powders and Porous Solids (Second Edition)*, F. Rouquerol, et al., Editors. 2014, Academic Press: Oxford. p. 237-268.
60. Kloss, S., et al., *Characterization of Slow Pyrolysis Biochars: Effects of Feedstocks and Pyrolysis Temperature on Biochar Properties*. Journal of environmental quality, 2012. **41**: p. 990-1000.
61. Jindo, K., et al., *Physical and chemical characterization of biochars derived from different agricultural residues*. Biogeosciences, 2014. **11**(23): p. 6613-6621.
62. Barrett, E.P., L.G. Joyner, and P.P. Halenda, *The Determination of Pore Volume and Area Distributions in Porous Substances. I. Computations from Nitrogen Isotherms*. Journal of the American Chemical Society, 1951. **73**(1): p. 373-380.
63. Sun, F., et al., *Controllable nitrogen introduction into porous carbon with porosity retaining for investigating nitrogen doping effect on SO₂ adsorption*. Chemical Engineering Journal, 2016. **290**: p. 116-124.
64. Zhou, Q., et al., *Preparation of high-yield N-doped biochar from nitrogen-containing phosphate and its effective adsorption for toluene*. RSC Advances, 2018. **8**(53): p. 30171-30179.
65. Anuwar, N. and P. Khamaruddin, *Optimization of Chemical Activation Conditions for Activated Carbon From Coconut Shell Using Response Surface Methodology (RSM) and Its Ability to Adsorb CO₂*. 2020.
66. Nandiyanto, A.B.D., R. Oktiani, and R. Ragadhita, *How to Read and Interpret FTIR Spectroscopy of Organic Material*. Indonesian Journal of Science and Technology, 2019. **4**(1): p. 97.
67. Lee, J.W., et al., *Characterization of Biochars Produced from Cornstovers for Soil Amendment*. Environmental Science & Technology, 2010. **44**(20): p. 7970-7974.
68. Moreno-Jiménez, E., et al., *The effect of biochar amendments on phenanthrene sorption, desorption and mineralisation in different soils*. PeerJ, 2018. **6**.
69. Rey-Maull, C.A., et al., *Comparative study of the adsorption of acetaminophen on activated carbons in simulated gastric fluid*. SpringerPlus, 2014. **3**(1): p. 48.
70. Chaves Fernandes, B.C., et al., *Impact of Pyrolysis Temperature on the Properties of Eucalyptus Wood-Derived Biochar*. Materials, 2020. **13**(24): p. 5841.
71. Shaheen, S.M., et al., *Wood-based biochar for the removal of potentially toxic elements in water and wastewater: a critical review*. International Materials Reviews, 2019. **64**(4): p. 216-247.
72. Zhang, H., R.P. Voroney, and G.W. Price, *Effects of temperature and processing conditions on biochar chemical properties and their influence on soil C and N transformations*. Soil Biology and Biochemistry, 2015. **83**: p. 19-28.
73. Pipiška, M., et al. *Biochar from Wood Chips and Corn Cobs for Adsorption of Thioflavin T and Erythrosine B*. Materials, 2022. **15**, DOI: 10.3390/ma15041492.
74. Bubici, S., et al., *Evaluation of the surface affinity of water in three biochars using fast field cycling NMR relaxometry*. Magnetic Resonance in Chemistry, 2016. **54**(5): p. 365-370.
75. Yuan, Y. and T.R. Lee, *Contact Angle and Wetting Properties*. 2013, Springer Berlin Heidelberg. p. 3-34.
76. Nguyen, B.T., et al., *Temperature Sensitivity of Black Carbon Decomposition and Oxidation*. Environmental Science & Technology, 2010. **44**(9): p. 3324-3331.

77. Zama, E.F., et al., *The role of biochar properties in influencing the sorption and desorption of Pb(II), Cd(II) and As(III) in aqueous solution*. Journal of Cleaner Production, 2017. **148**: p. 127-136.
78. Chen, X., et al., *Adsorption of copper and zinc by biochars produced from pyrolysis of hardwood and corn straw in aqueous solution*. Bioresource Technology, 2011. **102**(19): p. 8877-8884.
79. Vaughn, S.F., et al., *Physical and chemical characterization of biochars produced from coppiced wood of thirteen tree species for use in horticultural substrates*. Industrial Crops and Products, 2015. **66**: p. 44-51.
80. Fang, Q., et al., *Aromatic and Hydrophobic Surfaces of Wood-derived Biochar Enhance Perchlorate Adsorption via Hydrogen Bonding to Oxygen-containing Organic Groups*. Environmental Science & Technology, 2014. **48**(1): p. 279-288.
81. Rattanakam, R., et al., *Assessment of Hydrophilic Biochar Effect on Sandy Soil Water Retention*. Key Engineering Materials, 2017. **751**: p. 790-795.

Figures



Figure 1

Wood samples divided into cubes prior to combustion



Figure 2

Crucible placement inside the furnace

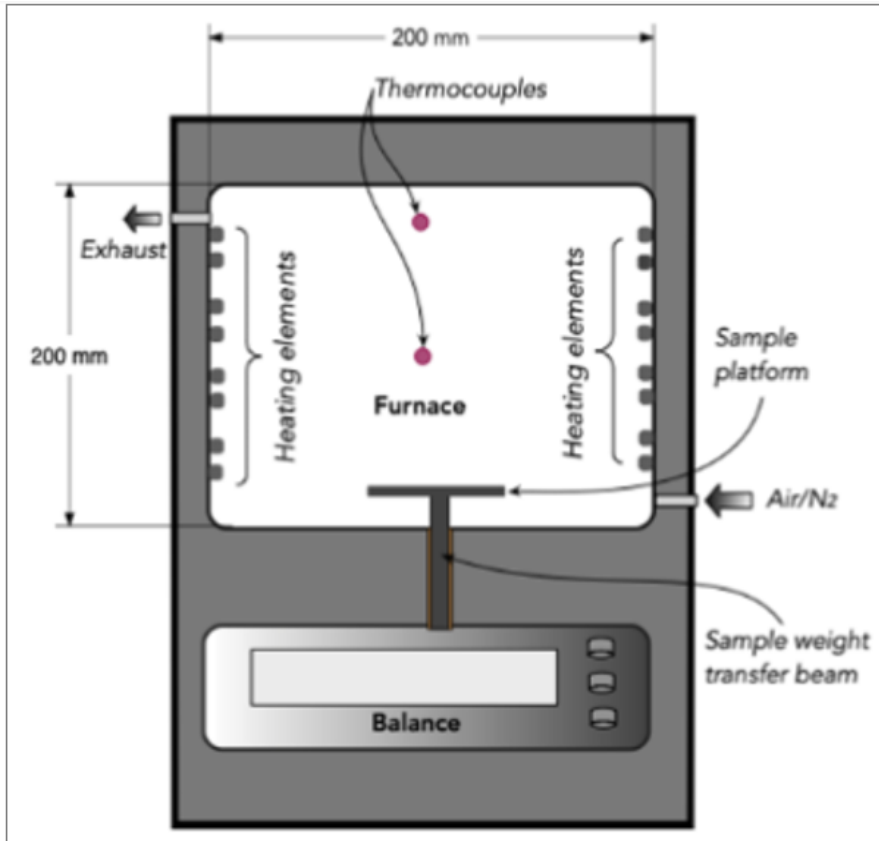


Figure 3

Schematic diagram of muffle furnace equipped with a weighing system (Cao et al., 2021)

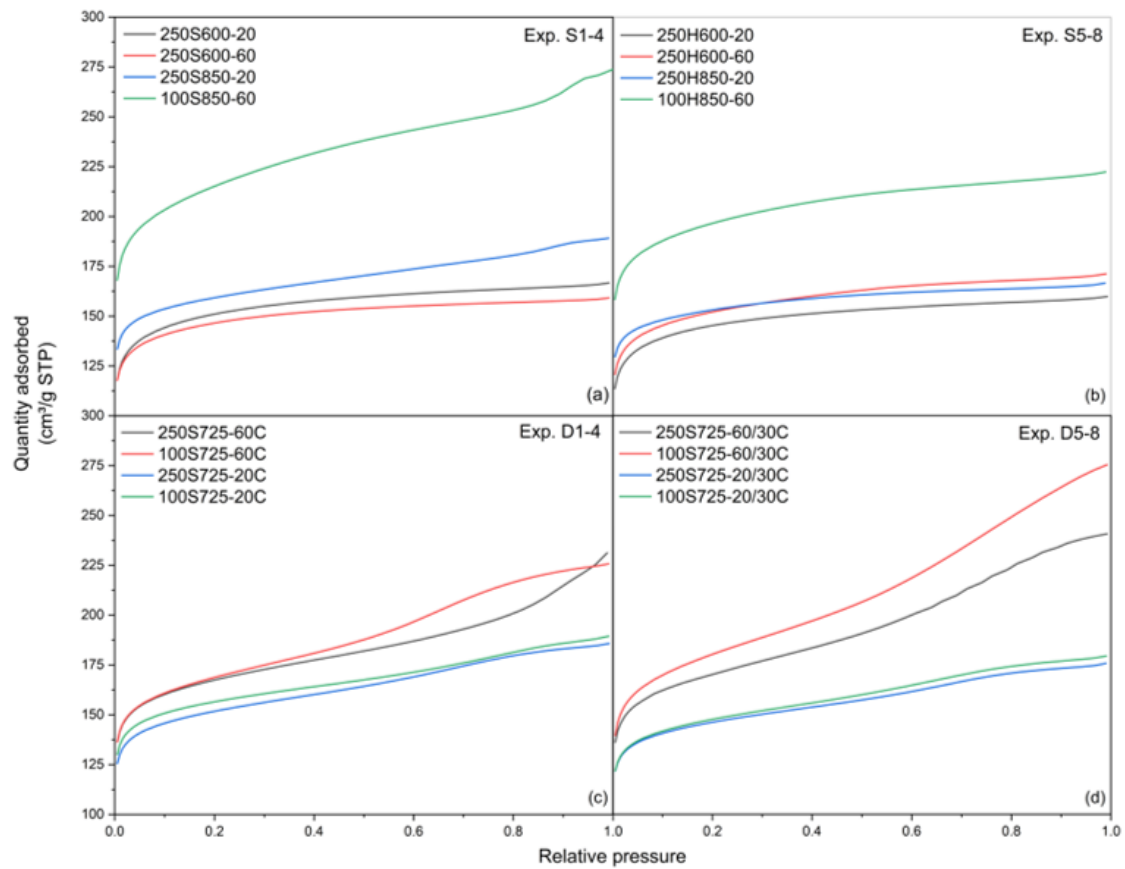


Figure 4

Adsorption isotherms obtained for biochars

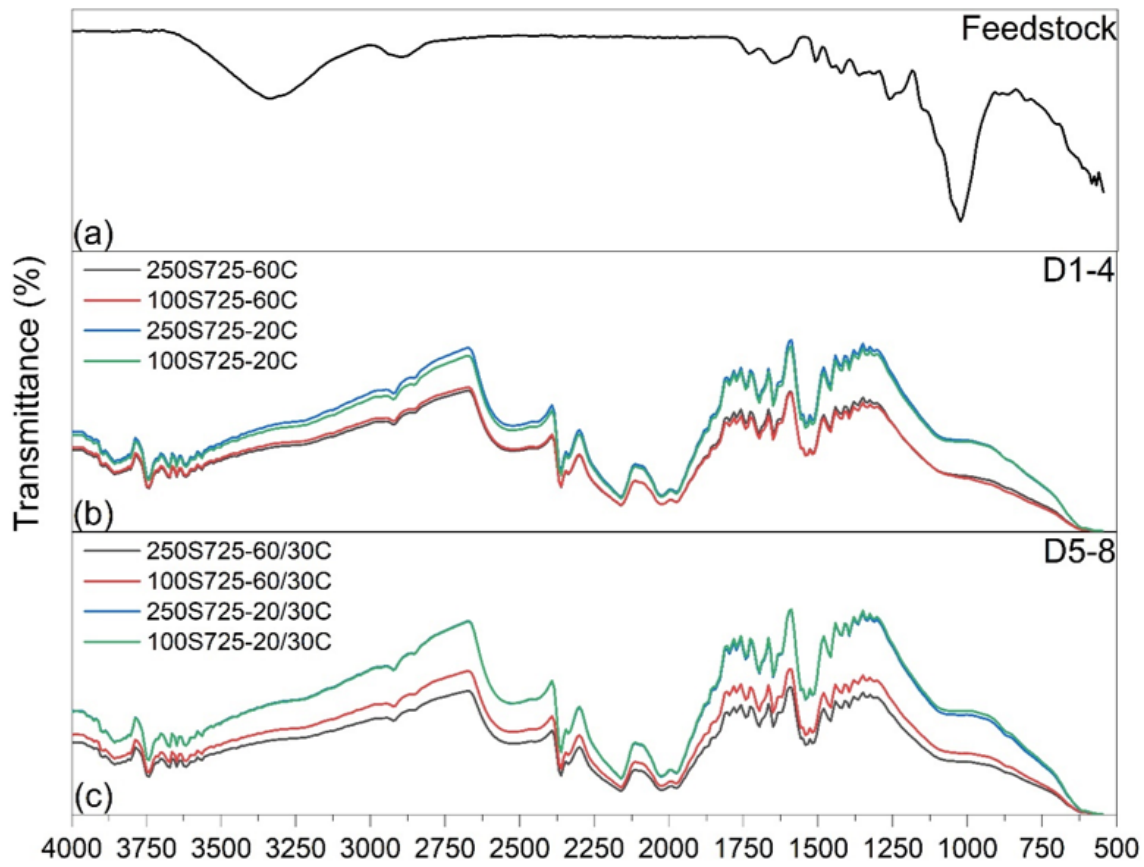


Figure 5

FTIR spectrum of feedstock and DoE biochars

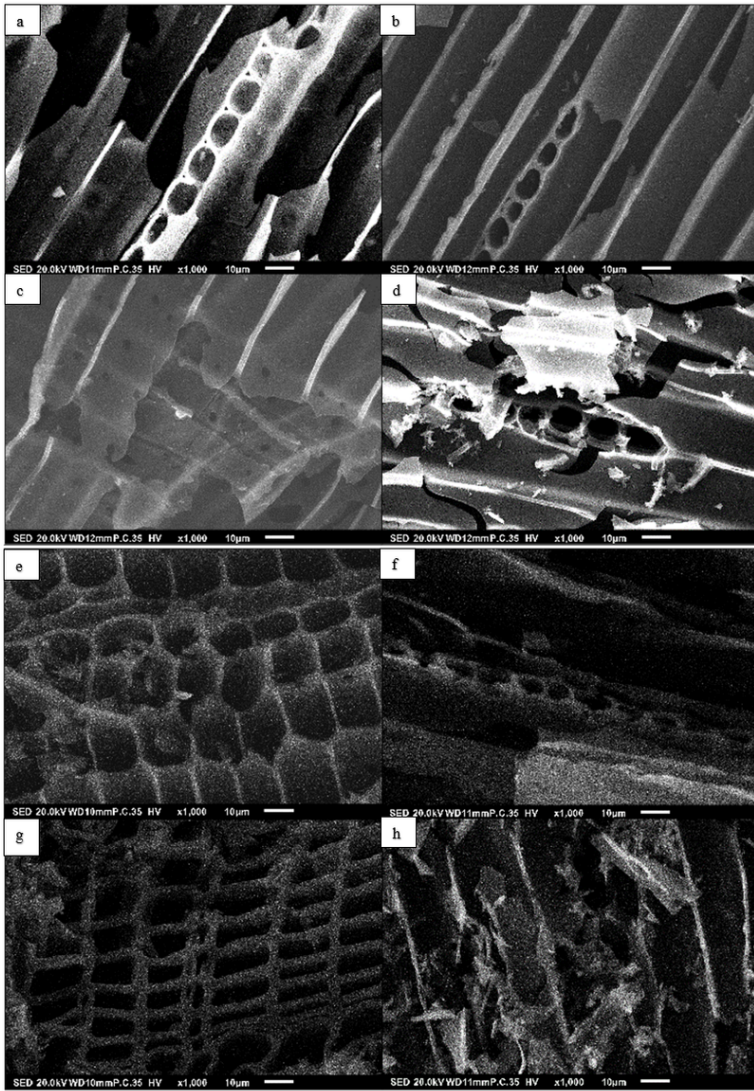


Figure 6

a-d - SEM of biochars with lower ramp rates; e-h SEM of biochars with higher ramp rates

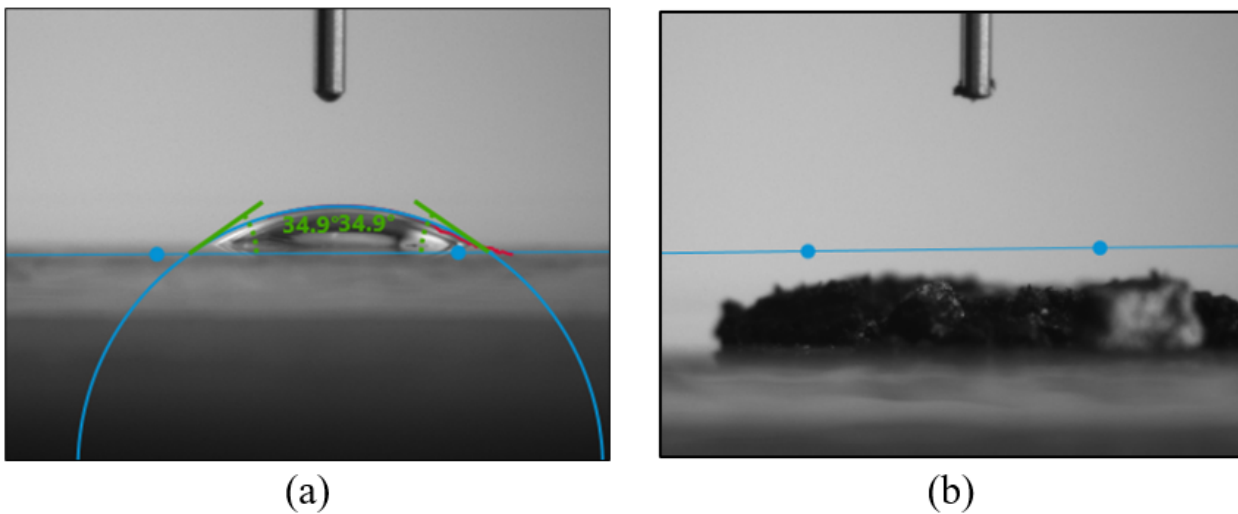


Figure 7

(a) Water droplet on a clear glass slide

(b) Water droplet on biochar surface